Inductive Electronegativity Scale. Iterative Calculation of Inductive Partial Charges

Artem Cherkasov*

Division of Infectious Diseases, Faculty of Medicine, University of British Columbia, 2733, Heather Street, Vancouver, British Columbia, V5Z 3J5, Canada

Received July 18, 2003

A number of novel QSAR descriptors have been introduced on the basis of the previously elaborated models for steric and inductive effects. The developed "inductive" parameters include absolute and effective electronegativity, atomic partial charges, and local and global chemical hardness and softness. Being based on traditional inductive and steric substituent constants these 3D descriptors provide a valuable insight into intramolecular steric and electronic interactions and can find broad application in structure−activity studies. Possible interpretation of physical meaning of the inductive descriptors has been suggested by considering a neutral molecule as an electrical capacitor formed by charged atomic spheres. This approximation relates inductive chemical softness and hardness of bound atom(s) with the total area of the facings of electrical capacitor formed by the atom(s) and the rest of the molecule. The derived full electronegativity equalization scheme allows iterative calculation of inductive partial charges on the basis of atomic electronegativities, covalent radii, and intramolecular distances. A range of inductive descriptors has been computed for a variety of organic compounds. The calculated inductive charges in the studied molecules have been validated by experimental *C-1s* Electron Core Binding Energies and molecular dipole moments. Several semiempirical chemical rules, such as equalized electronegativity's arithmetic mean, principle of maximum hardness, and principle of hardness borrowing could be explicitly illustrated in the framework of the developed approach.

INTRODUCTION

Historically, chemical practice mostly relied on empirical rules and accumulated experimental results rather then mathematically descriptive solutions. Nowadays, quantum physics can relate many properties of a molecule with its spatial structure using comprehensive terms of fundamental laws governing microworld. Methods of quantum chemistry become closely integrated into chemical and biochemical practice and find wider use in planning and executing of new compounds and experiments. Nonetheless, a broad practical use of accurate theoretical methods is still not feasible in many areas of research, especially for describing biological activity of compounds. The reason for that is not only in unbearable computational cost of quantum calculations for larger molecular systems but also an inability of quantum methods to describe behavior of chemicals in the macroworld of fluids and biopolymers. Ultimately, drug designers and medicinal chemists still have to operate by empirical rules and semiempirical or statistical models allowing evaluation of properties of compounds in terms of formal quantitative structure−activity relationships (QSAR).[1]

Modern areas of the QSAR use a broad range of atomic and molecular characteristics called descriptors varying from purely empirical (such as hydrophobicity, polarizability, substituent constants, etc.) to merely theoretical descriptors related to the quantum energy.[2] These two extreme classes of QSAR variables both have great importance for practice and both suffer from similar drawbacks. Empirical parameters are adequate in describing biological activity but may require actual experimental determination and often do not possess clear physical meaning, while physically meaningful quantum descriptors can only be accessed through complicated and time-consuming quantum-chemical procedures. Thus, finding ways to compute empirical and quantum QSAR variables from readily accessible atomic or molecular parameters or other QSAR descriptors is an important task for modern QSAR methodology.

RESULTS AND DISCUSSION

Our previous studies have demonstrated that very basic characteristics of bound atoms such as their electronegativities, covalent radii, and interatomic distances can be sufficient for interpretation of numerous important group and molecular properties and can provide informative insights into intra- and intermolecular interactions.[3−6] Using these properties we have developed quantitative models for accurate calculation of substituent inductive and steric constants—empirical descriptors which have originated the modern area of the QSAR.

Thus, in the framework of a model of frontal steric effect the steric influence R_S of substituent G toward a reaction center RC can be calculated as a sum of *relative* areas of radial shadows shielded by atoms of the G on RC's spherical surface (see Figure 1 and its caption)[3]:

$$R_{sG\rightarrow RC} = \alpha \sum_{i\subset G}^{n} \frac{R_i^2}{r_{i-RC}^2} \qquad (1)$$

Here α is a calibration constant, R_S is the steric substituent constant, n is the number of atoms in the substituent, R_i is

* Corresponding author phone: (604)875-4111 x68541; fax: (604)875-4013; e-mail: artc@interchange.ubc.ca.

10.1021/ci034147w CCC: $25.00
Published on Web 10/14/2003

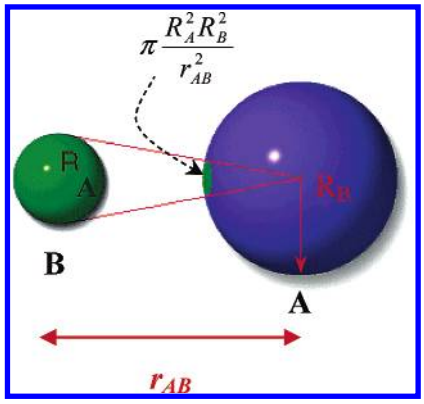

Figure 1. Radial shielding on spherical surface of atom *A* by the neighboring atom *B*. The area of a frontal of a surface of atom *A* by atom *B* (shown as a green shadow) is $\pi\frac{R_A^2 R_B^2}{r_{AB}^2}$. The entire area *A* is πR_A^2, thus the relative screened surface of *A* can be determined as $\frac{S_{shadow}}{S_{atom}} = \frac{\pi R_A^2 R_B^2}{\pi R_A^2 r_{AB}^2} = \frac{R_B^2}{r_{AB}^2}$.

the radius of the *ith* atom, and r_{i-RC} is the direct distance between the *ith* atom and the atom-reaction center *RC*. The area of frontal screening of a surface of atom A by atom B (shown as a green shadow in Figure 1) can be calculated as

$$\pi\frac{R_A^2 R_B^2}{r_{AB}^2}$$

and the *relative* screened surface of *A* is determined as

$$\frac{S_{shadow}}{S_{atom}} = \frac{\pi R_A^2 R_B^2}{\pi R_A^2 r_{AB}^2} = \frac{R_B^2}{r_{AB}^2}$$

It has been established that R_S steric parameters calculated for common organic substituents formed a high quality correlation with the corresponding Taft's empirical E_S-steric constants ($N = 35$, $R^2 = 0.985$).[3,7]

Similar methodology has been developed in the framework of a model of inductive effect also using atomic consideration of inductive substituent parameters:[4]

$$\sigma^*_{G\to RC} = \beta\sum_{i\subset G}\frac{\Delta\chi^0_{i-RC} R_i^2}{r_{i-RC}^2} \qquad (2)$$

Here σ^* is a Taft's inductive constant of substituent *G* at the reaction center *RC* (in initial approximation considered as sp^3-hybridized carbon atom), *n* is a number of atoms in the *G*, r_i is the distance between the *ith* atom and the *RC*, $\Delta\chi_{i-RC}$ is the difference in absolute inductive electronegativities of the *ith* atom and the *RC* (the driving force for the electron density displacement), and R^2 is the surface of the *ith* atom of substituent (reflecting its ability to delocalize partial charge). The theoretical inductive σ^* constants calculated for *427* common substituents by formula 2 have formed with the corresponding experimental numbers a perfect correlation with *0.99* coefficient.[3,4]

The developed quantitative models 1 and 2 allowed us to approach numerous important theoretical problems associated with that of inductive and steric interactions, such as inductive and steric influence of alkyl substituents,[8,9] inductive and steric effects in organometallic chemistry,[10] substituent effect in the chemistry of free radicals,[11−13] substituent effect on energy of covalent bonds,[14] possible dependence between substituent constants and electronegativity,[5] and partial charges and chemical hardness−softness.[6] A new method of quantification of substituent effect, called "Three Dimensional Correlation Analysis", has been elaborated on the basis of eqs 1 and 2 allowing accurate prediction of an extensive data set of dissociation constants of carboxylic acids and protonated amines.[15] By fitting the experimental inductive constants within (2) we have also established a scale of inductive electronegativities χ_i^I for a broad range of atoms in different valent states.[8]

In the present work the models of inductive and steric effects and inductive electronegativity scale have been further developed for calculation of novel "inductive" descriptors − atomic partial charges, in situ atomic − and group electronegativity, local and global chemical hardness and softness. It was anticipated that these developments will lead to novel prospective 3D QSAR descriptors and useful relationships between quantum QSAR descriptors and empirical substituent constants.

Molecule as Nanoscale Capacitor. In our previous studies[3] we have used analogies with the theory of electrostatic induction to relate inductive partial charges occurring on interacting atoms *A* and *B* with their mutual inductive influence:

$$\Delta N_A \approx \sigma^*_{A\to B} - \sigma^*_{B\to A}$$

Using this approximation we could express a partial charge ΔN_A occurring on atom *A* due to its inductive interaction with atom *B* as the following:

$$\Delta N_A = \frac{\Delta\chi^0_{B-A} R_B^2 - \Delta\chi^0_{A-B} R_A^2}{r_{B-A}^2} = \frac{\Delta\chi^0_{B-A}(R_B^2 + R_A^2)}{r_{B-A}^2} \qquad (3)$$

On the basis of correlation with the experimental bond dipole moments we have introduced the normalization coefficient into eq 3 to provide ΔN the dimension of elementary charge [e][3]:

$$\Delta N_A = 0.172\frac{\Delta\chi^0_{B-A}(R_B^2 + R_A^2)}{r_{B-A}^2} \qquad (4)$$

(here *R* and *r* are taken in Angstroms [Å]).

The interpretation of the developed eq 4 for inductive partial charges can be elaborated in terms of a model of nanoscale capacitance. This model approximating interacting atoms as spherical metallic (jellium) particles have been used in numerous charge calculation methods reported to date.[16−21]

Using such approximation we can speculate that the difference in atomic electronegativities will determine the potential of the uniform electric field between charged spheres A and B:

$$U_{AB} \approx \frac{\chi_B}{r_{AB}} - \frac{\chi_A}{r_{BA}}$$

It is known that electric charge accumulated in a capacitor with facings A and B is described as $q = C_{AB}U_{AB}$ where C_{AB} is a nanoscale capacitance of the system.[22] Thus, if we express eq 3 for the inductive partial charge as the following

$$\Delta N_A = \frac{\Delta\chi_{B-A}}{r_{AB}}\frac{(R_A^2 + R_B^2)}{r_{AB}} = U_{B-A}\frac{(R_A^2 + R_B^2)}{r_{AB}}$$

then the term

$$\frac{(R_A^2 + R_B^2)}{r_{AB}}$$

can be corresponded with a capacitance C_{AB} of a nanoscale capacitor AB.

The classic formula of an electric capacitance $C = \epsilon\epsilon_0(S/d)$ includes the total area of capacitor's facings ($\boldsymbol{S}$) and is the distance between the facings ($\boldsymbol{d}$).[22] Assuming that the facings of a nanoscale capacitor are formed by spherical surfaces of atoms A and B we can relate $\boldsymbol{d}$ with the distance between atoms A and B r_{AB} and $\boldsymbol{S}$ with the overall area of the surfaces of the interacting atoms $S_{AB} = (R_A^2 + R_B^2)$.

The extent of distribution of electron density occurring between two interacting atoms can then be interpreted as a charge accumulated between the facings of a nanoscale electric capacitor formed by the spherical surfaces of atoms and powered by the difference in their electronegativities.

The nanoscale capacitor model is a clear simplification considering atoms as metallic spheres and omitting the order of interatomic connections. It should be noted, however, that the exact topology of chemical bonds may not have an effect on full electronegativity equalization which occurs over the entire molecule. In other words, to share their electronegativity two atoms do not have to be connected directly by a bond, they just have to be connected into the same molecular skeleton. This way, each atom shares its electronegativity with all other atoms of molecule. Thus, for a polyatomic system the inductive charge occurring on the *ith* atom can be calculated from the corresponding pair-wise interactions of i with all other atoms j

$$\Delta N_i = 0.172\sum_{j\neq i}^{N-1}\frac{\Delta\chi_{j-i}(R_j^2 + R_i^2)}{r_{j-i}^2} \qquad (5)$$

(where N is the number of atoms in molecule).

Equation 5 operating by atomic electronegativities, radii, and intramolecular distances can be readily evaluated by simple matrix algebra and, thus, can be used for calculating gas-phase partial charges even in larger molecular systems. The examples of such calculations will be present in the later sections.

The underlying capacitance model can also be used to define useful analogies between (5) and important quantum descriptors associated with the concept of electronegativity equalization. Numerous previous studies[16,20,21,23−28] have identified possible linkage between charge capacitance and chemical hardness and softness—the parameters quantified within the Density Functional Theory (DFT). The authors have used electrical capacitance as intuitive justification for chemical softness as charge delocalizing ability and described useful analogies between mathematical apparatus of traditional electrostatics and the DFT.[16,21,28]

Using equations for inductive charge and capacitance and definitions of the DFT we have approached the quantification of "inductive" analogues of chemical hardness and softness.

Equalization of Inductive Electronegativity. Within the DFT[23] the equalized (in situ) electronegativity χ' of a bound atom is defined by its partial charge ΔN and unmodified ("absolute") atomic electronegativity χ^0 and hardness η^0

$$\chi' = \chi^0 + \eta^0\Delta N \qquad (6)$$

where the local chemical hardness η^0 reflects the "resistance" of electronegativity to a change of the atomic charge. The definition of absolute chemical hardness has been introduced by Pearson who has associated it with deformation of the electron cloud in the course of binding.[24]

The development of a modern concept of chemical hardness and softness has to a large extent been determined by the studies of Parr and Pearson and co-workers. Within the scope of the DFT Parr and co-workers draw the fundamentally important analogy between electronegativity and an electron chemical potential, which has the same value throughout the molecular system and is determined as the partial derivative of the energy E with respect to the number of electrons at the constant external potential V_{eff}:

$$-\chi \approx \left.\frac{\partial E}{\partial N}\right|_{V_{eff}}$$

Subsequently, Parr and Pearson[25] determined the second derivative of the energy with respect to the number of electrons as absolute hardness

$$\eta \approx \frac{1}{2}\left.\frac{\partial^2 E}{\partial^2 N}\right|_{V_{eff}} \approx -\frac{1}{2}\left.\frac{\partial\chi}{\partial N}\right|$$

and the change in the number of electrons with respect to a change of electronegativity as chemical softness s:

$$s = \frac{1}{\eta} \approx -2\frac{\partial N}{\partial\chi}$$

Applying this transformation to eq 5 we can derive the inductive atomic softness of atom i as a partial derivative of its inductive charge with respect to χ_i

$$s_i = -2\frac{\partial q_i}{\partial\chi_i} = 2\sum_{j\neq i}^{N-1}\frac{R_j^2 + R_i^2}{r_{j-i}^2} \qquad (7)$$

(the normalizing coefficient are omitted in (7) and the later formulas).

Thus, the inductive atomic softness of a bound atom can be defined as a *relative* area of frontal shadows screened on its surface by the rest of the molecule. According to the model of frontier steric effect (1) inductive chemical softness can be addressed as total steric interaction occurring between atom and the rest of the molecule:

$$s_i = 2(R_{S_{i\rightarrow MOL}} + R_{S_{MOL\rightarrow i}})$$

The inductive chemical hardness of atom *i* can be defined as the inversed parameter:

$$\eta_i = \frac{1}{2\sum_{j\neq i}^{N-1} \frac{R_j^2 + R_i^2}{r_{j-i}^2}} = \frac{1}{(R_S + R_S)} \quad (8)$$

The "geometric" definitions 7 and 8 also relate inductive local hardness−softness with the total area of the facings of nanoscale capacitor formed by this atom and the rest of the molecule. The global inductive softness s_{MOL} of *N*-atomic molecule can, in turn, be expressed as a sum of all *relative* areas of radial shadows formed by the constituent atoms (sort of an effective inner surface of a molecule):

$$S_{MOL} = \sum_{j\neq i}^{N}\sum_{j\neq i}^{N} \frac{R_j^2 + R_i^2}{r_{j-i}^2} = \sum_{j\neq i}^{N} 2\frac{R_j^2 + R_i^2}{r_{j-i}^2} = \sum_{i}^{N} S_i \quad (9)$$

Such analogy provides explicit illustration for chemical softness of an atom as its ability to delocalize (store) partial charge. The definition 9 also justifies the known condition of atomic additivity of the chemical softness.

Thus, the developed eqs 5 and 7−9 allow estimating quantitative analogues of such important quantum QSAR descriptors as local and global hardness and softness through basic and readily accessible properties of bound atoms—their covalent radii and interatomic distances. These relationships can also be used to calculate the equalized (in situ) inductive electronegativity χ'. The combination of eq 6 for in situ electronegativity with the formulas for inductive atomic charge (5) and inductive local hardness (8) allows expressing χ' as the following:

$$\chi'_i = \chi_i^0 + \eta_i q_i = \chi_i^0 + \frac{\sum_{j\neq i}^{N-1} \frac{(\chi_j^0 - \chi_i^0)(R_j^2 + R_i^2)}{r_{j-i}^2}}{2\sum_{j\neq i}^{N-1} \frac{R_j^2 + R_i^2}{r_{j-i}^2}} \quad (10)$$

Considering that electronegativity of the *ith* atom χ_i^0 is a constant term for summation over other *N−1* atoms of molecule we get the equation

$$\chi'_i = \chi_i^0 + \frac{\sum_{j\neq i}^{N-1} \frac{\chi_j^0(R_j^2 + R_i^2)}{r_{j-i}^2}}{2\sum_{j\neq i}^{N-1} \frac{R_j^2 + R_i^2}{r_{j-i}^2}} -$$

$$\frac{\chi_i^0}{2} \leftrightarrow \chi'_i = \frac{\chi'_i}{2} + \frac{1}{2}\frac{\sum_{j\neq i}^{N-1} \frac{\chi_j^0(R_j^2 + R_i^2)}{r_{j-i}^2}}{\sum_{j\neq i}^{N-1} \frac{(R_j^2 + R_i^2)}{r_{j-i}^2}} \quad (11)$$

Table 1. Inductive Group Electronegativities of Some Common Substituents Calculated by Eq 12 and the Corresponding χ Values Reported in the Literature

substituent	$\chi_{IND.}$	χ^{30}	χ^{31}	χ^{32}	χ^{33}	χ^{34}
F	4.00	3.90	4.00	4.00	10.01	3.98
CH_2F	2.50	2.61			4.97	
Cl	3.28	3.00	3.07	3.47	7.65	3.16
CH_2Cl	2.40	2.47			4.89	
$CHCl_2$	2.61	2.63				
Br	3.13	2.68	2.81	3.22		2.96
CH_2Br	2.40	2.79				
$CHBr_2$	2.60	2.40				
I	2.93		2.47	2.78		2.66
CH_2I	2.38	2.79				
OH	2.91	3.53	2.85	2.80	6.96	3.46
CH_2OH	2.34				4.14	2.45
OCH_3	2.69		2.42	2.51	5.73	3.40
OC_2H_5	2.62					3.39
SH	2.62	2.35	2.27	2.47	5.69	2.65
CH_2SH	2.28				3.39	
SCH_3	2.49				4.99	
NH_2	2.46	2.82	2.39	2.48	6.16	3.10
R^a		0.868	0.981	0.988	0.978	0.802

[a] Correlation coefficients between inductive group electronegativities and presented χ-scales.

Here we need to make the important assumption that the last summation term in (11) can be associated with an absolute group electronegativity of the rest of the molecule χ^0_{MOL-i}:

$$\chi^0_{MOL\rightarrow i} = \frac{\sum_{j\neq i}^{N-1} \frac{\chi_j^0(R_j^2 + R_i^2)}{r_{j-i}^2}}{\sum_{j\neq i}^{N-1} \frac{(R_j^2 + R_i^2)}{r_{j-i}^2}} \quad (12)$$

This approximation allows us to define the effective (in situ) electronegativity of atom *i* in the molecule as the arithmetic mean of its unchanged absolute electronegativity χ_i^0 and absolute electronegativity of the rest of the molecule χ^0_{MOL-i}:

$$\chi'_i = \frac{\chi_i^0 + \chi^0_{MOL-i}}{2}$$

Such definition of inductive effective electronegativity of a bound atom coincides with the arithmetic mean principle used by Sanderson to originate the electronegativity equalization concept.[29]

To evaluate the adequacy of the introduced inductive group electronegativity we have calculated χ^0_G values of a number of common organic substituents considered to be attached to a *C-sp*^{3} reaction center. The corresponding parameters are present in Table 1 along with group electronegativity values from other scales.[30−34]

As can be seen for the data, the obtained group inductive parameters χ_G correlate well with some previously published electronegativity scales with correlation coefficients of 0.97−0.98. A reasonable agreement (correlation coefficients 0.80−0.86) was found with other scales. Noticeably, better quality

Table 2. Iterative Accumulation of Partial Atomic Charges and Equalization of Effective Electronegativities in the CH_3F Molecule

iteration	C	H	F
0	$s(C) = 2*0.172*\left(\frac{3*(0.30^2+0.77^2)}{1.09^2}\Big/\frac{(0.77^2+0.64^2)}{1.35^2}\right) = 0.78$	$s(H) = 2*0.172*\left(\frac{(0.30^2+0.77^2)}{1.09^2}\Big/\frac{(0.30^2+0.64^2)}{2.00^2}\Big/2*\frac{(0.30^2+0.30^2)}{1.78^2}\right) = 0.28$	$s(C) = 2*0.172*\left(\frac{3*(0.30^2+0.64^2)}{2.00^2}\Big/\frac{(0.77^2+0.64^2)}{1.35^2}\right) = 0.32$
	$\eta(C) = 1.28$ $\chi^0(C) = 2.20$	$\eta(H) = 3.57$ $\chi^0(H) = 2.10$	$\eta(F) = 3.14$ $\chi^0(F) = 4.00$

iteration	*q(C)*	*χ(C)*	*q(H)*	*χ(H)*	*q(F)*	*χ(F)*
1	0.141	2.388	0.051	2.281	−0.292	3.079
2	0.177	2.427	0.078	2.377	−0.410	2.709
3	0.189	2.442	0.090	2.420	−0.458	2.558
4	0.194	2.448	0.094	2.438	−0.478	2.495
5	0.196	2.450	0.097	2.446	−0.486	2.470
6	0.196	2.451	0.098	2.449	−0.490	2.459
7	0.196	2.451	0.098	2.450	−0.491	2.455
8	0.196	2.451	0.099	2.451	−0.491	2.453
8	0.196	2.451	0.099	2.451	−0.492	2.452
9	0.197	2.452	0.099	2.452	−0.492	2.452

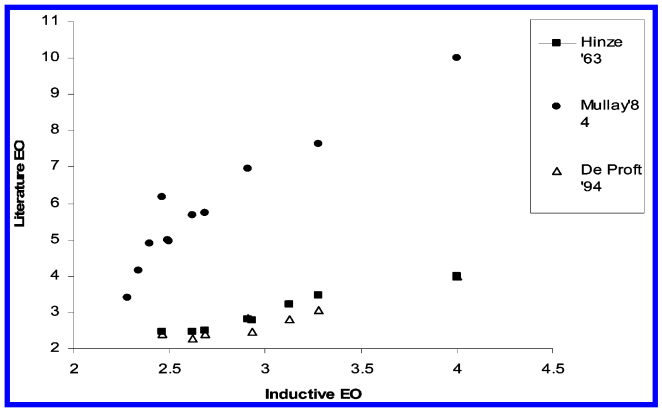

Figure 2. Dependence between "inductive" and some literature electronegativity scales.

correlations have been established with electronegativities of quantum chemical origin[31−33] (illustrated by Figure 2).

It is expected that eq 12 can also be used for the simple calculation of absolute group electronegativity from atomic χ values within any known atomic electronegativity scale. For this purpose, the carbon-atom can be suggested as the hypothetical rection center for the calculation of r_i-parameters in (12). It should be elaborated, that the developed simple method of calculation of group electronegativities takes into account a real spatial structure of the substituent and, thus, allows differentiating χ of isomeric fragments and also makes it possible to explore the dependence of electronegativity of the substituent on its conformation.

Iterative Calculation of Inductive Partial Charges. The reported developments demonstrate the fact that relatively simple mathematical procedures operating by easily accessible atomic parameters can not only be used for calculation of empirical QSAR descriptors (such as inductive and steric substituent constants) but also allow quantification of important quantum QSAR variables such as partial charges, hardness, and effective electronegativity. For larger molecular systems the developed approaches can produce inductive partial charges and equalized atomic electronegativities calculated in a stepwise iterative manner. The example of such an iterative calculation is presented in Table 2 for the CH_3F molecule.

At each iterative step of the calculation eq 5 has been applied to define atomic charge increment $\Delta\Delta N$ from effective atomic electronegativities χ' established by the previous iteration (χ^0 for the initial iteration):

$$\Delta\Delta N_{i+1} = 0.172\sum_{j\neq i}^{N-1}\frac{\Delta\chi'_{j-i}(R_j^2+R_i^2)}{r_{j-i}^2} \qquad (13)$$

The calculated charge increment is, in turn, used to produce the next iterative value of effective atomic electronegativity:

$$\chi'_{i+1} = \chi'_i + \eta_i q_i = \chi'_i + \frac{\Delta\Delta N}{2\sum_{j\neq i}^{N-1}\frac{(R_j^2+R_i^2)}{r_{j-i}^2}} \qquad (14)$$

The repetitive usage of eqs 13 and 14 has been carried out until electronegativities of all atoms of the CH_3F molecule acquire the same χ' value. The total cumulative partial charge on each atom has then been expressed as a sum of all incremental contributions $\Delta N_i = \sum_k \Delta\Delta N_i$ estimated by k iterations. The gradual equalization of electronegativities of constituent *H*, *C*, and *F* atoms in the CH_3F molecule is illustrated by Figure 3.

Using the developed iterative charge calculation approach (13) we have attempted to reproduce a number of experimental parameters reflecting charge separation in covalently bound molecules. Thus, on the basis of eq 14 we have calculated "inductive" charges on hydrogen atoms in a series of hydrogen halides molecules HX. Estimated values of *q(H)* are presented in Table 3 along with the dipole moments of the corresponding hydrogen halides molecules μ, reduced to l - bond lengths of HX.

The values μ/l, reflecting the distribution of electron density in hydrogen halides molecules, form the correlation of high

Table 3. Inductive Charges and Reduced Dipole Moments for Halogen Halide[a]

molecule	$\chi(X)$	$R(X)$ [A]	$r\ (HX)$ [A]	$\mu/_l$ [D/A]	$q(H)$ [e]	$\eta(H)$	$\eta(HX)$	$\chi'(HX)$
HF	4.00	0.64	0.84	2.09	0.2314	3.79	1.89	3.10
HCl	3.28	0.99	1.2	0.81	0.1508	3.29	1.65	2.74
HBr	3.13	1.14	1.33	0.56	0.1392	3.08	1.54	2.67
HI	2.93	1.33	1.52	0.26	0.1149	2.97	1.48	2.57

[a] Hydrogen radii and "inductive" electronegativity have been taken as 0.30 A and 2.10, respectively.

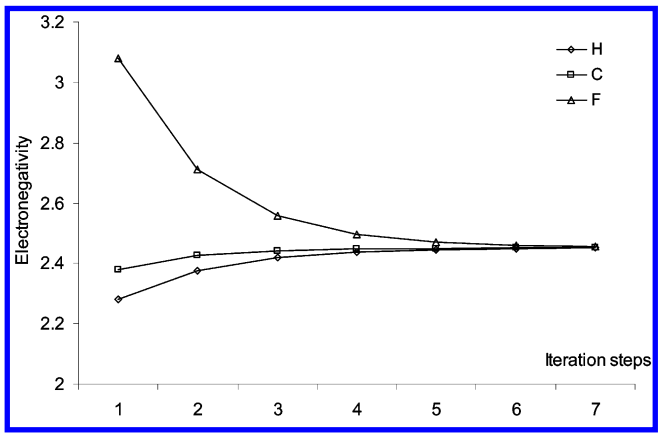

Figure 3. Equalization of inductive electronegativity of bound C, H, and F atom in the *CH_3F* molecule during iterative calculation of inductive partial charges.

quality ($r^2 = 0.998$) with the calculated "inductive" charges *q(H)* on hydrogen atoms. The corresponding dependence is presented in Figure 4 graphically.

The inductive quantum descriptors have also been calculated for the series of halogen-substituted methanes CH_4, CH_3F, CH_2F_2, CF_4, CH_3Cl, CH_2Cl_2, $CHCl_3$, CCl_4, CH_3Br, CH_2Br_2, $CHBr_3$, CBr_4, CH_3J, CF_3Cl, CF_3Br, and CF_3J. These compounds have been previously used in the work of *Gasteiger* and *Marsili*[35] to evaluate the calculation of partial charges through iterative partial equalization of orbital electronegativities. The authors used experimental *C-1s* core electron binding energies for these compounds as the most unambiguous measure of partial atomic charges on their carbon atoms. We have also correlated the exact same experimental *C-1s* core binding energies taken from ref 36 with the cumulative inductive charges *q(C)* calculated by iterative usage of (13) and (14) and collected into Table 4. The linear dependence between the inductive charges and the corresponding carbon core binding energies in the series of the halogen-substituted methanes is presented in Figure 5.

The established correlation coefficient $r = 0.980$ is comparable with the value $r = 0.993$ reported by *Gasteiger* and *Marsili*. However, unlike the partial orbital electronegativity equalization procedure (and many other similar approaches based on electronegativity equalization) the developed methodology of calculation of inductive partial charges (13) takes into account the real three-dimensional structure of the molecule. Operating by easily accessible atomic electronegativities, radii, and interatomic distances, the "inductive" scheme can become a useful tool for electrostatic simulations for large molecular systems.

We have also used calculated inductive charges to compute dipole moments of the substituted halogen methanes which then have been compared with the corresponding experimental μ. The experimental and calculated parameters are also present in Table 4. The correlation between the two sets is present in Figure 6.

It should be mentioned that the experimental values of the dipole moments taken from ref 37 may have significant experimental errors. While most of the dipole moment values in Table 4 are for the liquid phase, some (marked with *) are for the gas phase (we used the recommended dipole moment when available, otherwise we took liquid-phase data for the widest range of temperatures; if nothing else was

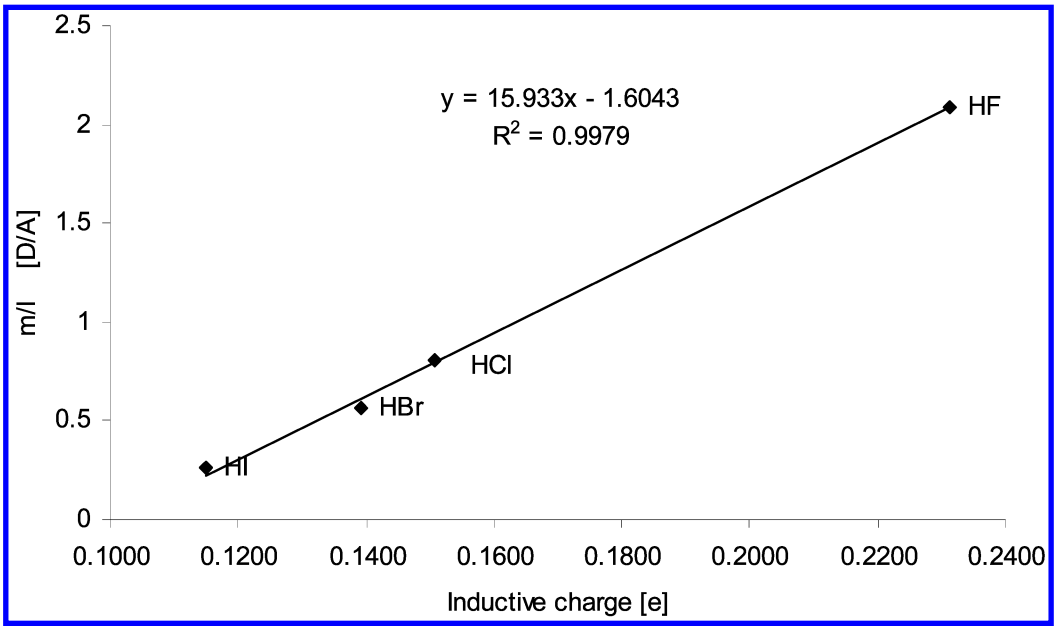

Figure 4. Dependence between the reduced dipole moments and inductive charges on hydrogen atoms in the series of halogen halides.

Table 4. Inductive QSAR Descriptors for Halogens Substituted Methanes

	C		H		Hal		molecule					
molecule	*q(C)*	*η(C)*	*q(H)*	*η(H)*	*q(Hal)*	*η(Hal)*	η_{mol}	χ'_{mol}	*C-1s* exper	*C-1s* predict	*μ* exper	*μ* calc
CH_4	−0.043	1.26	0.011	4.22			1.15	2.14	290.9	289.85	0	0
CH_3F	0.197	1.28	0.098	3.57	−0.491	3.14	1.03	2.45	293.7	292.47	1.82	1.82
CH_2F_2	0.430	1.29	0.198	3.30	−0.413	3.00	0.98	2.75	296.44	294.97	2.102[a]	1.96
CHF_3	0.666	1.31	0.302	3.19	−0.323	2.88	0.94	3.07	299.24	297.44	1.82[a]	1.62
CF_4	0.894	1.32			−0.224	2.76	0.91	3.38	301.85	299.91	0	0
CH_3Cl	0.114	1.31	0.075	3.31	−0.340	2.73	0.98	2.35	292.48	291.63	1.94	1.94
CH_2Cl_2	0.253	1.36	0.154	2.88	−0.280	2.63	0.91	2.54	294	293.17	2.24	1.9
$CHCl_3$	0.385	1.41	0.251	2.55	−0.212	2.53	0.87	2.74	295.1	294.65	1.94	1.26
CCl_4	0.521	1.46			−0.130	2.44	0.86	2.96	296.39	296.16	0	0
CH_3Br	0.101	1.31	0.072	3.20	−0.318	2.51	0.95	2.33	292.12	291.48	1.79	1.79
CH_2Br_2	0.223	1.35	0.147	2.72	−0.259	2.42	0.87	2.50	292.8	292.84	2.06	1.85
$CHBr_3$	0.340	1.40	0.242	2.36	−0.194	2.35	0.83	2.67	293.7	294.15	1.79	1.21
CBr_4	0.462	1.45			−0.115	2.27	0.82	2.87	294.81	295.50	0	0
CH_3J	0.077	1.30	0.065	3.09	−0.272	2.31	0.92	2.30	291.43	291.21	1.3	1.48
CF_3Cl	0.803	1.35			−0.269 (*F*)	2.65 (*F*)	0.89	3.29	300.31	299.01	0.12[a]	0.39
					0.003 (*Cl*)	2.58 (*Cl*)						
CF_3Br	0.790	1.35			−0.282 (*F*)	2.60 (*F*)	0.87	3.27	299.33	298.87	0.029[a]	0.58
					0.056 (*Br*)	2.42 (*Br*)						
CF_3I	0.795	1.35			−0.286 (*F*)	2.54 (*F*)	0.85	3.27	299	298.63	0.52[a]	0.92
					0.063 (*I*)	2.27 (*I*)						

[a] Mark values of the gas-phase dipole moments.

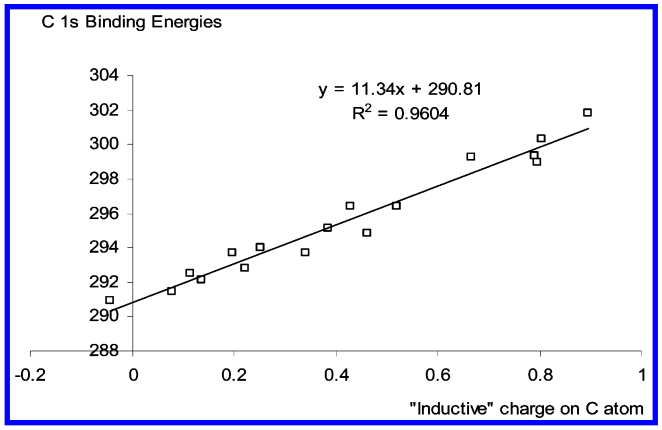

Figure 5. *C-1s* bonding energies of halogens substituted methanes versus inductive partial charges on C atoms.

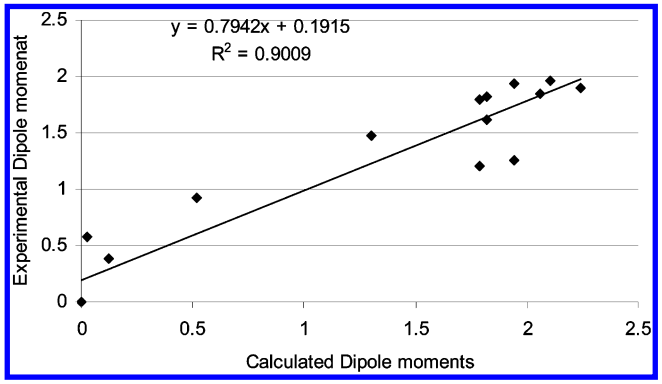

Figure 6. Dependence between the experimental dipole moments of a series of halogen substituted methanes and the corresponding values calculated from the inductive partial charges of the constituent atoms.

available the gas-phase numbers have been taken). Despite the ambiguity of the experimental values, the correspondence between the experimental and theoretical dipole moments is quite good with the correlation coefficient established as $r^2 = 0.90$. Most noticeable deviations from the linear trend in Figure 6 have been estimated for methanes substituted with multiple halogens. These deviations can be explained by strong halogen saturation effects in the corresponding molecules.

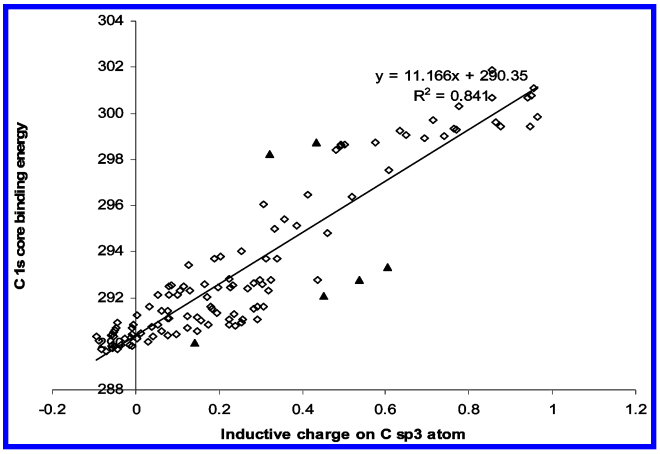

Figure 7. Dependence between experimental values of *C-1s* bonding energies and inductive charges on C sp3 atoms in a series of organic molecules.

We did not limit the validation of the approach by the data set used in a work of *Gasteiger* and *Marsili* and have calculated inductive partial charges on Csp3 atoms in a wide series of organic molecules containing a greater variety of atomic types. The computed inductive charges on Csp3 atoms are collected in Table 5 along with the corresponding experimental *C-1s* electron binding energies.

The established correlation between charges and core binding energies for the entire set of studied compounds (including halogen-methanes) is presented graphically in Figure 7.

The theoretical values of the *C-1s* electron core binding energies estimated from the correlation with the inductive charges are also collected in Tables 4 (for the substituted methanes) and 5 (for all other Csp3 containing molecules). Despite the fact that some observations clearly deviate from the general trend (points marked as black triangles in Figure 7) the estimated correlated coefficient $R = 0.917$ demonstrates a good applicability of eq 13 for the sake of partial

Table 5. *C-1s* Core Electron Binding Energies (Gas Phase) and Calculated Inductive Charges on C Sp3 Atom for Series of Organic Compounds[a]

name	*q (Csp3)*	*C-1s* predict	*C-1s* exper	name	*q (Csp3)*	*C-1s* predict	*C-1s* exper
$BrCH_2C(O)OCH_2C^*H_3$	0.25	293.18	290.9	$(CH_3SiH_2)_2S$	−0.06	289.73	290.4
$BrC^*H_2C(O)OCH_2CH_3$	0.27	293.36	292.38	$CF_3C{\equiv}CH_3$	0.71	298.33	299.7
CF_3OCl	0.85	299.88	300.67	$CF_3CH{=}CH_2$	0.43	295.18	298.72
CH_3SiH_2Cl	0.01	290.48	290.45	$CF_3C(O)OC^*H_3$	0.60	297.08	293.34
CF_2Cl_2	0.69	298.09	298.93	$C^*F_3C(O)OCH_3$	0.65	297.58	299.03
CH_3SiHCl_2	0.12	291.72	290.68	$CF_3CF{=}CF_2$	0.86	300.00	299.6
CCl_3F	0.61	297.14	297.54	$CF_3C(O)CF_3$	0.95	300.91	299.41
CH_3SiCl_3	0.24	293.02	290.79	$CH_3CH{=}CH_2$	−0.01	290.27	290.68
CH_3SiH_2F	0.06	291.05	290.53	$CH_3C(O)CH_3$	0.15	291.98	291.15
CH_3SiHF_2	0.22	292.86	290.8	$CH_2{=}CHOCH_3$	0.11	291.53	292.31
CH_3SiHI_2	0.08	291.20	290.37	$CH_3C(O)OC^*H_3$	0.24	292.99	291.3
CH_3OH	0.13	291.79	292.3	$C^*H_3C(O)OCH_3$	0.23	292.96	292.55
CH_3SH	0.06	291.05	291.41	$HC(O)OC^*H_2CH_3$	0.23	292.90	292.45
CH_3SiH_2I	−0.01	290.25	290.42	$HC(O)OCH_2C^*H_3$	0.23	292.86	291.04
CH_3NH_2	0.03	290.73	291.6	$(CH_3O)_2C(O)$	0.32	293.97	292.74
CH_3SiH_3	−0.09	289.29	290.31	$(CH_3)_2NC(O)H$	0.17	292.27	292.03
$C^*H_3CH_2Cl$	0.08	291.21	291.1	C_3H_8	−0.05	289.81	290.57
$CH_3C^*H_2Cl$	0.08	291.25	292.1	$(CH_3)_3SiI$	−0.01	290.19	289.95
$(CH_3)_2SiHCl$	0.00	290.40	290.24	$(CH_3)_3N$	0.00	290.38	291.26
$C^*H_3CHCl_2$	0.18	292.40	291.5	$ClCH_2C(O)OCH_2C^*H_3$	0.26	293.23	291.07
$CH_3C^*HCl_2$	0.20	292.64	293.8	$ClCH_2C(O)OC^*H_2CH_3$	0.28	293.52	292.64
$(CH3)_2SiCl_2$	0.10	291.44	290.4	$(CH_3)_3CCl$	0.05	290.93	290.8
$C^*H_3CCl_3$	0.28	293.50	291.5	$(CH_3)_3CCl$	0.05	290.93	292.13
$CH_3C^*Cl_3$	0.33	294.07	295	$(CH_3)_3SiC^*H_2Cl$	−0.01	290.27	290.83
CH_3CH_2F	0.13	291.75	291.19	$(C^*H_3)_3SiCH_2Cl$	−0.01	290.27	289.88
CH_3CH_2F	0.13	291.78	293.39	$FCH_2C(O)OCH_2C^*H_3$	0.29	293.60	291.06
$(CH_3)_2SiHF$	0.04	290.82	290.33	$FC^*H_2C(O)OCH_2CH_3$	0.31	293.85	293.7
CH_3SiHF_2	0.29	293.60	291.62	$FCH_2C(O)OC^*H_2CH_3$	0.30	293.74	292.58
CH_3SiHF_2	0.31	293.78	296.05	$CH_3C{\equiv}CCH_3$	0.14	291.93	290.03
C^*F_3COOH	0.77	298.95	299.28	$CH_3OC(O)CH{=}CH_2$	0.32	293.92	292.32
$C^*H_3CF_3$	0.45	295.39	292.07	$CH_3C(O)OC(O)CH_3$	0.36	294.33	295.4
$CH_3C^*F_3$	0.49	295.86	298.64	$CH_3C(O)OC^*H_2CH_3$	0.20	292.54	292.45
$CF_3C^*H_2OH$	0.54	296.34	292.77	C_4H_{10}	−0.05	289.77	290.48
$C^*F_3CH_2OH$	0.58	296.78	298.71	$(CH_3)_4Si$	−0.08	289.42	289.78
$CF_3C^*H_2NH_2$	0.44	295.23	292.77	$((CH_3)_2SiH)_2O$	−0.03	289.96	289.93
$C^*F_3CH_2NH_2$	0.48	295.71	298.42	$((CH_3)_2SiH)_2S$	−0.06	289.73	289.93
CF_3CF_3	0.96	301.12	299.85	$(CH_3)_3CC(O)Cl$	0.18	292.38	291.6
CF_3OCF_3	0.95	301.01	301.09	$CH_3C(O)OCl$	0.17	292.30	290.83
CF_3OOCF_3	0.95	300.94	300.78	$CH_3C^*H_2C(O)OCH_2CH_3$	0.17	292.20	292.6
CF_3OOOCF_3	0.94	300.84	300.69	$CH_3CH_2C(O)OCH_2C^*H_3$	0.16	292.11	291
CF_3SCF_3	0.87	300.11	299.41	$(C^*H_3)_4C$	−0.05	289.75	290.4
$CH_3C(O)H$	0.19	292.52	291.35	C_5H_{12}	−0.05	289.74	290.42
$CH_3C(O)OH$	0.31	293.77	291.6	cyclohexane	−0.05	289.77	290.3
$HC(O)OCH_3$	0.30	293.69	292.78	C_6H_{14}	−0.06	289.71	290.36
CH_3CH_3	−0.05	289.83	290.7	$[(CH_3)_3Si]_2O$	−0.04	289.86	289.76
$C^*H_3CH_2OH$	0.08	291.25	291.1	$[(CH_3)_3Si]_2S$	−0.05	289.74	289.79
$CH_3C^*H_2OH$	0.08	291.25	292.5	$[(CH_3)_3Si]_2NH$	−0.07	289.55	289.67
CH_3OCH_3	0.09	291.31	292.55	$CF_3C_6H_5$	0.32	293.94	298.24
CH_3SCH_3	0.04	290.79	290.74	$CH_3C_6H_5$	0.03	290.67	290.1
$(CH_3)_2SiHI$	−0.01	290.22	290.28	CF_3, $CF_3-C_6H_4$ m	0.50	295.95	298.64
$(CH_3)_2SiH_2$	−0.09	289.38	290.14	CF_3, $CF_3-C_6H_4$ p	0.49	295.85	298.58
$(CH_3SiH_2)_2O$	−0.03	290.06	290.2	$C_6H_4C(O)CH_3$	0.15	292.00	290.56

[a] Values used for the calculation: *Inductive electronegativity: χ(F) = 4.00; χ(Cl) = 3.28; χ(Br) = 3.13; χ(I) = 2.93; χ(H) = 2.10; χ(Csp3) = 2.20; χ(Csp2) = 2.31; χ(Csp2) = 3.15; χ(Osp3) = 3.20; χ(Osp2) = 4.34; χ(Si) = 1.99; χ(S) = 2.74; χ(N) = 2.59;* covalent radii: R(F) = 0.64; R(Cl) = 0.99; R(Br) = 1.14; R(I) = 1.33; R(H) = 0.30; R(Csp3) = 0.77; R(Csp2) = 0.67; R(Csp) = 0.60; R(Osp3) = 0.66; R(Osp2) = 0.60; R(Si) = 1.11; R(S) = 1.04; R(N) = 0.70.

charge calculation in organic molecules. Moreover, the analysis of the outliers revealed that all of them contain the CF3 group, and, thus, the corresponding calculated inductive charges most likely deviate due to the presence of the halogen saturation effect. If we delete these deviating points (CF_3OCF_3, $CF_3CH_2NH_2$, CH_3CF_3, CF_3CH_2OH, $CF_3CH{=}CH_2$, $CF_3C(O)OCH_3$, and $C_6H_5CF_3$) the correlation coefficient improves to $R = 0.942$.

Due to the absence of reliable numerical data on effective harness and molecular electronegativities it is difficult to access the accuracy of calculated inductive hardness η and equalized electronegativity χ' values presented in Table 4; we can only speculate that the established orders of these parameters for halogen substituted methanes seem to justify common chemical intuition. The calculated effective inductive hardness of hydrogen atoms in halogen halides presented in Table 3 also illustrate a known phenomenon of hardness borrowing implying that "the harder (smaller) the free atom (group) to which a hydrogen is attached, the harder the hydrogen is".[26] Such behavior can be easily understood in terms of eq 8 where a decrease of R_i leads to an increase of the corresponding hydrogen hardness η_H.

The introduced geometrical definition of inductive hardness also allows interpreting another well-recognized empirical rule of maximal chemical hardness introduced by Pearson.[38,39] It is well-understood that in the absence of additional stabilizing factors, any molecular system tends to its least shielded geometry hence decreasing the magnitude of the summarized mutual steric influence. Therefore, according to (9) the magnitude of the global molecular hardness will tend to its maximal possible value substantiating the principle of maximal hardness.

Summarizing, it is possible to conclude that the developed approaches demonstrate definite adequacy while calculating quantum QSAR descriptors for small molecules and allow for illustrating several useful semiempirical rules for electronegativity and chemical hardness. The elaborated models can be used as a convenient method for calculation of empirical and quantum QSAR descriptors from readily available parameters of bound atoms and considered as real three-dimensional structures of molecules.

CONCLUSIONS

On the basis of the previously developed models for inductive and steric effect we have introduced new QSAR descriptors: inductive analogues of chemical hardness (softness), absolute and effective electronegativity, and partial atomic charge.

The developed approaches define important quantitative relationships between purely empirical substituent constants and descriptors of quantum chemical origin and allow calculation of σ^*, R_S, χ^0, q, η, s, and χ' on the basis of atomic electronegativities, covalent radii, and interatomic distances.

The elaborated inductive descriptors can be readily calculated for molecular systems of any size, and thus they may become a useful tool for quantification of intramolecular interactions within large sets of chemical compounds as well as in proteins and other macromolecules. The fact that the developed inductive parameters are related to the experimentally determined inductive and steric constants provides an important empirical justification for these novel 3D QSAR descriptors.

REFERENCES AND NOTES

(1) *3D QSAR in Drug Design*; Kubinyi, H., Folkers, G., Martin, Y. C., Eds.; Kluwer: Dordrecht, 2002.
(2) Karelson, M. *Molecular Descriptors in QSAR/QSPR*, Wiley: New York, 2000; p 448.
(3) Cherkasov, A. R.; Galkin, V. I.; Cherkasov, R. A. *Russ. Chem. Rev.* **1996**, *65*, 641.
(4) Cherkasov, A. R.; Galkin, V. I.; Cherkasov, R. A. *J. Phys. Org. Chem.* **1998**, *11*, 437.
(5) Cherkasov, A. R.; Galkin, V. I.; Cherkasov, R. A. *J. Mol. Struct. (THEOCHEM)* **1999**, *489*, 43.
(6) Cherkasov, A. R.; Galkin, V. I.; Cherkasov, R. A. *J. Mol. Struct. (THEOCHEM)* **2000**, *497*, 115.
(7) Galkin, V. I.; Sayakhov, R. D.; Cherkasov, R. A. *Russ. Chem. Rev.* **1991**, *60*, 1617.
(8) Cherkasov, A. R.; Galkin, V. I.; Sibgatullin, I. M.; Cherkasov, R. A. *Russ. J. Org. Chem.* **1997**, *33*, 11320.
(9) Cherkasov, A. R.; Galkin, V. I.; Cherkasov, R. A. *Russ. J. Org. Chem.* **1995**, *31*, 1362.
(10) Galkin, V. I.; Cherkasov, A. R.; Cherkasov, R. A. *Phosph., Silicon, Sulf.* **1999**, *146*, 329.
(11) Cherkasov, A.; Jonsson, M. *J. Chem. Inf. Comput. Sci*. **1998**, *38*, 1151.
(12) Cherkasov, A.; Jonsson, M. *J. Chem. Inf. Comput. Sci*. **1999**, *39*, 1057.
(13) Cherkasov, A. R.; Jonsson, M.; Galkin, V. I. *J. Mol. Graph. Model.* **1999**, *17*, 28.
(14) Cherkasov, A.; Jonsson, M. *J. Chem. Inf. Comput. Sci*. **2000**, *40*, 1222.
(15) Cherkasov, A.; Sprous, D.; Chen, R. 3D Correlation Analysis − A Novel Approach to the Quantification of Substituent Effects. *J. Phys. Chem. A.* **2003**, in press.
(16) Sabin, J. R.; Trickey, S. B.; Apell, S. P.; Oddershede. J. *Int. J. Quantum Chem*. **2000**, *77*, 358.
(17) Huheey, J. E. J. *J. Phys. Chem.* **1965**, *69*, 3284.
(18) Evans, S.; Huheey, J. E. J. *J. Chem. Phys. Lett*. **1973**, *19*, 114.
(19) Ray, N. K.; Samuels, L.; Parr R. G. *J. Chem. Phys*. **1979**, *70*, 3680.
(20) Komorowski, L. *J. Chem. Phys.* **1987**, *114*, 55.
(21) Perdew, J. P. *Phys. Rev. B.* **1988**, *37*, 6175.
(22) Zisman, G. A.; Todes, O. M. *General Physics;* Nauka: Moscow, 1972; Vol. 2, p 234.
(23) Parr, R. G.; Yang, W. *Density-functional theory of atoms and molecules*; Oxford University Press: New York, 1989.
(24) Pearson, R. G. *J. Am. Chem. Soc.* **1963**, *85*, 3533.
(25) Parr, R. G.; Pearson, R. G. *J. Am. Chem. Soc.* **1983**, *105*, 7512.
(26) Huheey, J. E. *J. Org. Chem.* **1971**, *36*, 204.
(27) Huheey, E. J.; Watts, J. C. *Inorg. Chem.* **1971**, *10*, 1553.
(28) Iafrate G. J.; Hess K.; Krieger J. B.; Macucci M. *Phys. Rev. B* **1995**, *52*, 10737.
(29) Sanderson, R. T. *Science* **1951**, *114*, 670.
(30) Sanderson, R. T. *J. Am. Chem. Soc.* **1983**, *105*, 2259.
(31) De Proft, F.; Amira, S.; Choho, K.; Geerling, P. *J. Phys. Chem*. **1994**, *98*, 5227.
(32) Hinze, J.; Whitehead, M. A.; Jaffe, H. H. *J. Am. Chem. Soc.* **1963**. *85*, 148.
(33) Mullay, J. *J. Am. Chem. Soc*. **1984**, *106*, 5842.
(34) Pauling, L. *The Nature of the Chemical Bond*, 3rd ed.*;* Cornell University Press: New York, 1960.
(35) Gastaiger, J.; Marsili, M. *Tetrahedron* **1980**, *36*, 3219.
(36) Jolly, W. L.; Bomben, K. D.; Eyermann, C. J. *Data Nuclear Data Tables* **1984**, *31*, 433.
(37) McCellan, A. L. *Tables of Experimental Dipole Moments*; W. H. Freeman & Co.: 1963; 713p.
(38) Pearson, R. W. *J. Chem. Educ.* **1987**, *64*, 561.
(39) Pearson, R. W. *Acc. Chem. Res.* **1993**, *26*, 250.

CI034147W